

Effect of Thickness on Structural, Morphological, and Optical Properties for Nanocrystalline Thin Films of Cd_{1-x}Sn_xS, for Optoelectronic Applications

Lamia K. Abbas*  

Department of Physics, College of science, University of Baghdad, Baghdad, Iraq.

*Corresponding Author.

Received 03/11/2023, Revised 11/12/2023, Accepted 13/12/2023, Published Online First 20/01/2024



© 2022 The Author(s). Published by College of Science for Women, University of Baghdad.

This is an Open Access article distributed under the terms of the [Creative Commons Attribution 4.0 International License](https://creativecommons.org/licenses/by/4.0/), which permits unrestricted use, distribution, and reproduction in any medium, provided the original work is properly cited.

Abstract

Thin films of Sn_{1-x}Cd_xS nanocrystals (X=0,0.7, and 1) with different thicknesses 200, 300, and 400 nm were prepared on glass bases at 300 °C by the participation method and chemical spray pyrolysis method (CSP). The effect of the concentration of Sn and thickness on the structural and optical properties of the prepared films was studied. The films were characterized to evaluate the structure, transmittance, and optical energy band gap. X-ray diffraction (XRD) studies showed that the films were polycrystalline with hexagonal and orthogonal structures. XRD and atomic force measurement results showed that the grain size increases with its thickness. The optical band gap energies and optical transmission and absorption types of the membranes were determined from the optical transmittance spectra. Optical absorption studies in the wavelength range 200-1100 nm showed that the energy gap values of the films decrease from 2.48-1.95 eV, 2.41-1.92 eV, and 2.3- 1.89 eV with increasing Sn concentration and with increase the thickness 200, 300, and 400 nm respectively. The best properties of the prepared material were determined for its possible use in the manufacture of solar cells

Keywords: Cd_{1-x}Sn_xS nanocrystalline, CdS nanoparticle, Chemical spray pyrolysis, Sn, Thin films.

Introduction

There is considerable interest in the field of transparent semiconducting materials such as CdS, SnS, etc. for use in a variety of applications, including architectural windows, solar cells, heat reflectors, light transparent electrodes, thin-films photovoltaic devices, and many other optoelectronic devices¹. CdS and SnS are both promising materials for solar cells. CdS, which belongs to II-VI compound semiconductors^{2,3}, is an n-type semiconductor with a direct band gap of (2.4eV), CdS is used as a window material for heterojunction

thin films solar cells⁴⁻⁸. It has also applications in light-emitting diodes (LED), gas detectors photovoltaic cells, nonlinear optics, and thin film transistors^{7,9,10}. SnS is one of the Tin chalcogenide layered semiconductors in group IV-VI, SnS, SnSe is a promising material for solar energy conversion^{11, 12}. SnS films are highly suitable for any application in several of solid-state devices, such as photovoltaic, photoelectrochemical(PEC), photoconductive cells, and intercalation battery systems^{13,14}. In addition, SnS thin films have a large optical absorption coefficient (> 10⁴ cm⁻¹)¹³⁻¹⁵. It

is a p-type window layer heterojunction device¹⁶⁻¹⁸. SnS materials have an optical energy gap for direct transitions of 1.6 eV.

Various methods employed for the deposition of CdS and SnS films are chemical bath deposition^{19, 20}, chemical vapour deposition¹, electrochemical deposition²¹⁻²³, rf sputtering, vacuum evaporation¹, and spray pyrolysis method^{24, 25}. Amongst all the deposition methods, the spray pyrolysis (SP) method is a simple, convenient, and low-cost

Materials and Methods

Cd_{1-x}Sn_xS nanocrystalline thin films were prepared on glass substrates at 300°C substrate temperature by the CSP method using aqueous solutions. The spray solution (prepared using the participant method) consisted of (by volume) 0.05M cadmium chloride (CdCl₂.H₂O), thiourea (H₂NCSNH₂), and 0.05 tin chloride (SnCl₂.2H₂O) solutions and sodium hydroxide (NaOH) to ensure maximum growth of medium alkaline. Tin solution or cadmium solution or together Tin and cadmium acetate solutions were heated up by 45°C with magnetic stirring principle. The alkaline NaOH solution was then added drop by drop to reach 10 pH. The color of the CdS solution in 30 minutes was light yellow. Then its color grew darker as the reaction time rose until it changed completely from dark yellow to orange. The composition of Cd_{1-x}Sn_xS films changed from pure SnS to pure CdS (x=0, 0.7, and 1). The glass substrates were soaked

Results and discussion

Structural characterization

The structural properties of the Cd_{1-x}Sn_xS films have been investigated by XRD patterns. The XRD patterns of the samples are given in Fig. 1. The spectra have been obtained by scanning angle 2θ in the range from 20° to 60°. The existence of multiple eight diffraction peaks, and sulphide phases in the diffraction patterns indicates the polycrystalline nature of the Cd_{1-x}Sn_xS. It is seen that the crystallinity of the CdS films is better than that of other films. It should be noted that the XRD patterns exhibit clear dependence on Sn concentration. The CdS film has been crystallized in a hexagonal (JCPDS Card no:96-101-1055) with the preferential orientation of(002) as shown in Fig. 1a. The intensity of the peak corresponding to the CdS phase decreases as SnS concentration increases

method for large-area deposition of many binaries, ternary, and quaternary semiconducting films with varying anion and cation concentrations. In this study, thin films of Cd_{1-x}Sn_xS nanocrystals were prepared using the thermal chemical spray method and their structural and optical properties were studied by studying the effect of changing thickness on their properties to obtain the best properties, which we were able to use in the manufacture of solar cells.

in chromic acid, cleaned in isopropyl alcohol, rinsed in distilled water at each step, and dried in air. The chemical spray-head-to-substrate distance was fixed approximately at 30 cm. Nitrogen was used as the carrier gas during spraying. The glass substrates were heated by an electrical heater and control of substrate temperature was done using a chrome – alumel thermocouple. The thickness of the films was measured using the weighted method. The structural properties of the films were studied using XRD analysis and it was performed by a Rigaku X-ray diffractometer system using CuKα radiation with the wavelength of λ=1.5406Å. The morphological properties of the films were investigated using CSPMAA3000 AFM. Optical transmittance spectra of the films were carried out using the Shimadzu UV-160 (UV-Visible-NIR Spectrophotometer) system covering the spectral range from 200 to 1100 nm.

as shown in Fig.1.c The SnS phase becomes dominant with lower Cd content. The SnS film has been crystallized in an orthorhombic structure (JCPDS Card no: 96-900-8296) with the preferential orientation of (021) as shown. Describes the spectrum X-ray diffraction of films (SnxCd_{1-x}S) thin when changing thickness, as evidenced by the way that the increase in thickness leads to increase the height of the peaks and increase the intensity of which indicates that the change in thickness affects the installation of the film, and this is due to the difference in the number of atoms forming the film from one area to another. The crystallite size of all prepared samples was determined for three peaks with the greatest intensity based on the following Scherrer equation²⁶:

$$D = 0.9\lambda / \beta \cos\theta, \quad \text{--- 1}$$

Where λ is the wavelength of the x-ray (\AA), β is FWHM (radian) is the intrinsic full width at Half Maximum of the Peak and θ is the Bragg's diffraction angle of the respective XRD Peak. The dislocation density (δ) is calculated using²⁷ $\delta=1/D^2$. It is interesting to note that the crystallite size of $\text{Cd}_{1-x}\text{Sn}_x\text{S}$ thin films improves and the defects like

dislocation density decrease with the increase of film thickness. This may be due to the improvement in crystallinity in the films with the increase in film thickness. The crystallite size (D) and dislocation density (δ) for different thicknesses are shown in Table 1.

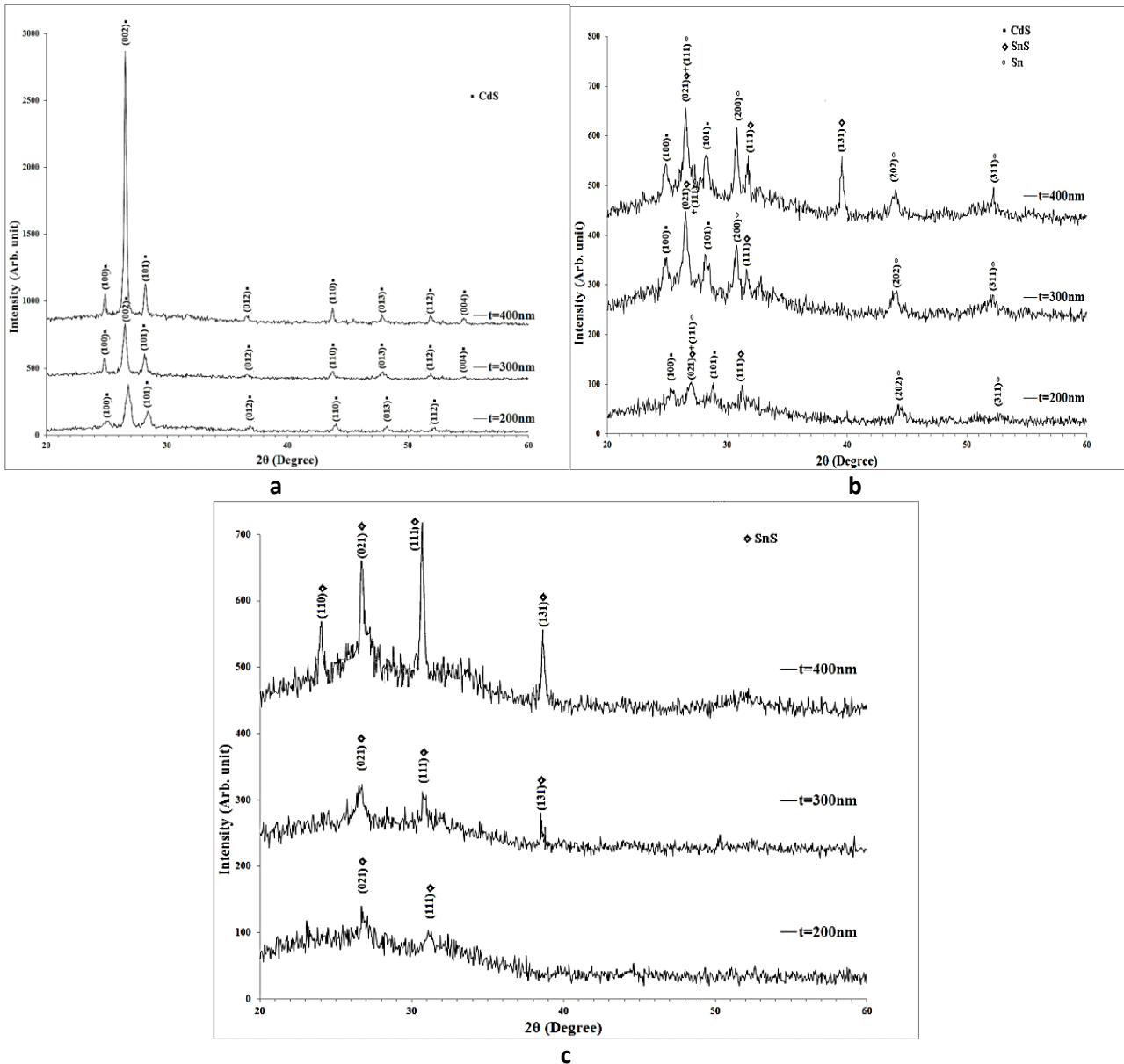


Figure1. a: XRD patterns of the CdS nanocrystall thin films of different thicknesses, b: XRD patterns of the $\text{Sn}_{0.7}\text{Cd}_{0.3}\text{S}$ nanocrystall thin films, c: XRD patterns of the SnS nanocrystall thin films of different thicknesses.

Table 1. Calculated values of the structural parameters of $Cd_{1-x}Sn_xS$ thin films of different thickness.

| Thin films | 2 θ (Deg.) | FWHM β (deg.) | crystallite size (nm) | δ $\times 10^{-3} m^{-2}$ | Thickness (nm) |
|----------------------|-------------------|---------------------|-----------------------|----------------------------------|----------------|
| CdS | 26.785 | 0.531 | 15.38 | 4.22 | 200 |
| | 26.558 | 0.354 | 23.06 | 1.88 | 300 |
| | 26.574 | 0.214 | 38.12 | 0.688 | 400 |
| Sn $0.7Cd_{0.3}S$ | 26.959 | 0.643 | 12.70 | 6.20 | 200 |
| | 26.474 | 0.468 | 17.43 | 3.29 | 300 |
| SnS | 26.515 | 0.468 | 17.44 | 3.28 | 400 |
| | 26.842 | 0.819 | 9.97 | 10.06 | 200 |
| | 26.649 | 0.936 | 8.72 | 13.15 | 300 |
| | 26.339 | 0.526 | 15.51 | 1.44 | 400 |

AFM technology provides digital images that quantitatively evaluate surface characteristics, including grain size (nm) and roughness average (nm). Fig. 2 demonstrates the spherical shapes for all samples studied. The images also show a non-compact surface which is not smooth. The grain size (average diameter) obtained from AFM measurements are listed in Table 2. The sizes of nanoparticles obtained from the AFM images appear bigger than the values obtained from XRD measurements²⁸. Those results can be interpreted for several reasons; the first explanation is that the nanoparticles tend to form aggregates on the surface during deposition. The second explanation is related

to the shape of the tip AFM which may cause misleading cross-sectional views of the sample. The results show that the grain size of CdS is larger than other samples which are consistent with X-ray results.

Table2. Variation of grain size and average diameter of $Cd_xSn_{1-x}S$ Nanocrystalline thin films with thickness of 400 nm

| nanocrystall films | Grain size(nm) | Avg. Diameter(nm) |
|---------------------|----------------|-------------------|
| CdS | 38.12 | 112.06 |
| $Cd_{0.3}Sn_{0.7}S$ | 17.44 | 117.03 |
| SnS | 15.51 | 99.59 |

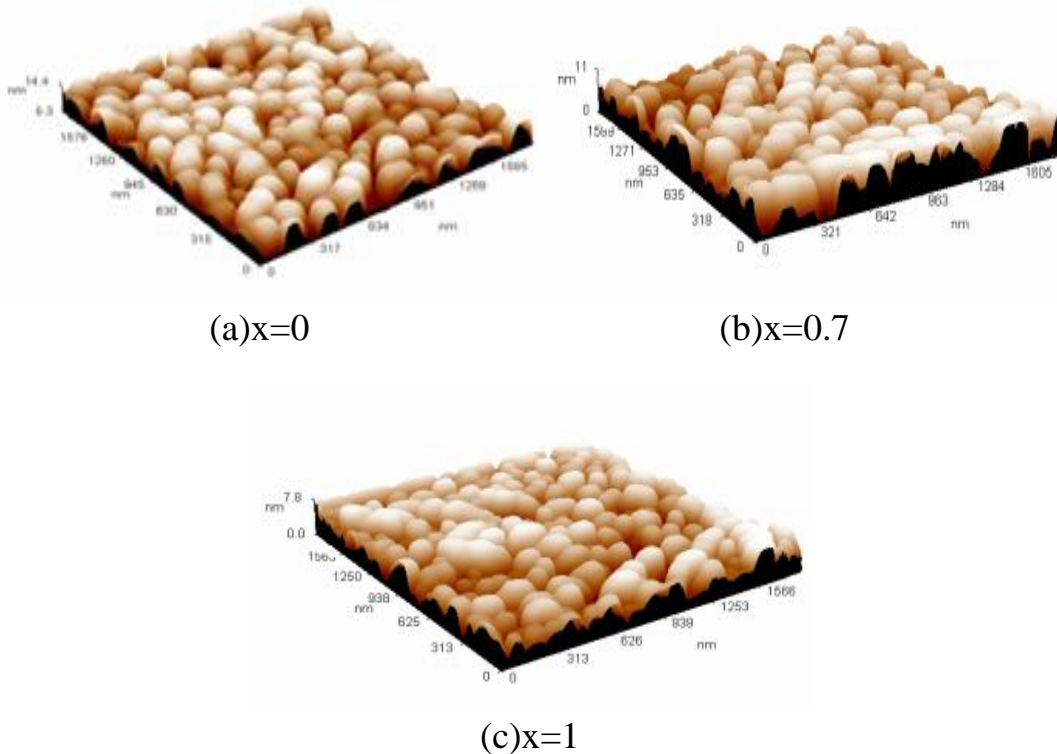


Figure 2. AFM micrographs of (a)CdS ,(b) Sn_{0.7}Cd_{0.3}S,(c)SnS Nanocrystalline thin films.

The optical properties of all films with different thicknesses 200,300 and 400 nm have been determined by using the transmittance (T) and absorbance (A) spectrum in the region (220-1100) nm.

The optical transmittance spectra of the prepared samples are shown in Fig. 3. The figure shows that the permeability decreases with increasing thickness for all prepared samples. The transmittance shows two distinct regions, first at short wavelengths of

less than 500 nanometers, where the transmittance suddenly increases with increasing wavelength. This phenomenon is attributed to the pack-pack transition, and the behavior of transitions appears directly in this region, while the second area, is larger than 500 nanometers. We notice that the curve tends to saturate. This is agreed upon by the researcher²⁹, as well as the researcher³⁰, while Fig. 4 shows the absorption spectrum.

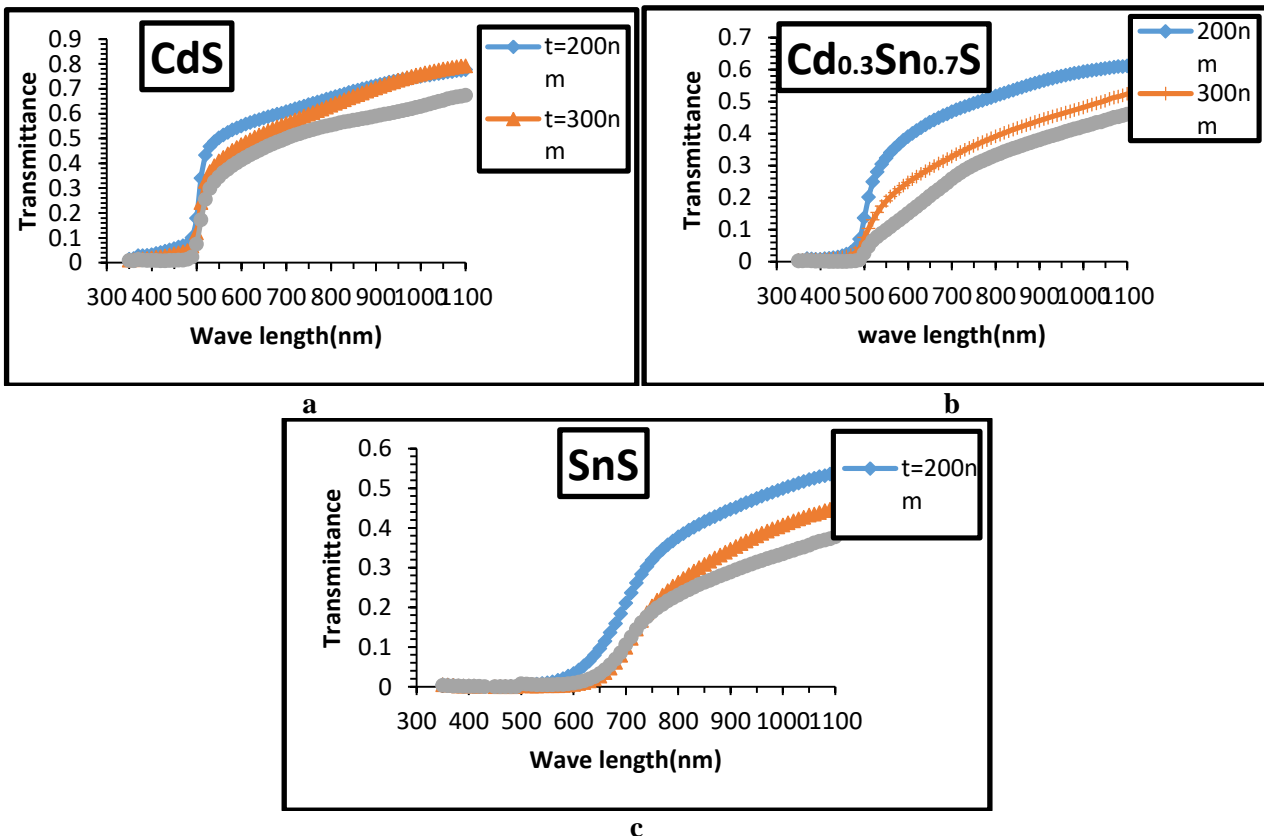
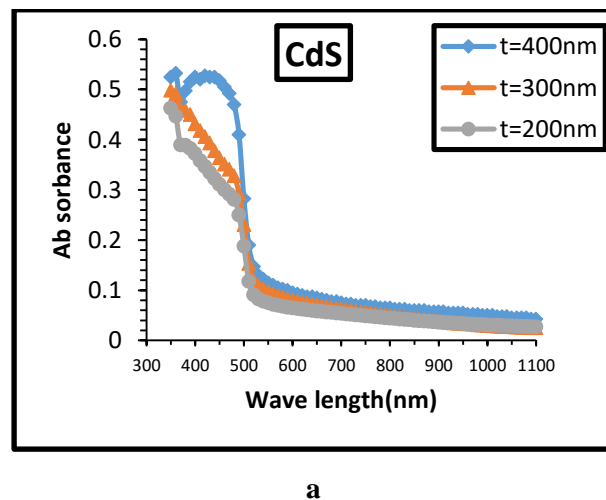


Figure 3. optical transmittance spectra of (a) CdS ,(b) Cd_{0.3}Sn_{0.7}S ,(c) SnS Nanocrystalline thin films with different thicknesses

The absorption spectra of Cd_{1-x}Sn_xS nanocrystalline thin films are shown in Fig. 3. It was observed that the absorption edge shifts towards longer wavelengths with increasing thickness, and this indicates a decrease in the energy gap with increasing thickness. Absorption increases with increasing thickness, and this is because increasing thickness increases the number of atoms, which provides absorption instances for many photons. It has been observed that after (400-500) nanometers there are no absorption peaks, and this stems from the high permeability of the membranes in the visible spectrum region, to observe the behavior. The opposite behavior of permeability. Agreed with the researcher²⁹.



a

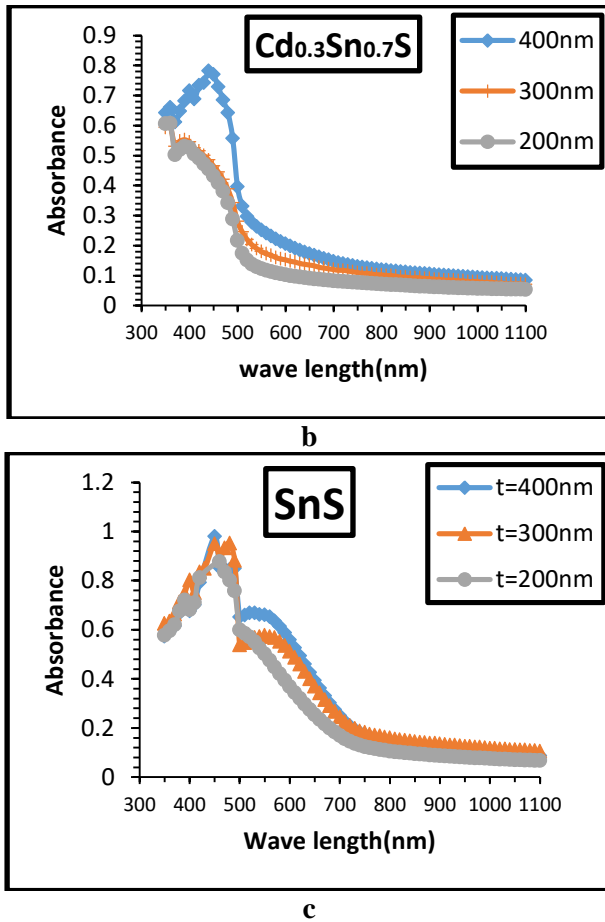


Figure 4. Optical absorption spectra of (a) CdS, (b) Cd_{0.3}Sn_{0.7}S, (c)SnS Nanocrystalline thin films with different thicknesses.

The absorption coefficient (α) associated with the strong absorption region of the films was calculated from absorbance (A) and the film thickness (t) using the relation: $\alpha = 2.3026 A/t$. The absorption coefficient of the Cd_{1-x}Sn_xS nanocrystalline films for the different thickness films increases with thickness as shown in Fig. 5.

The figure notes the value of the absorption coefficient was ($\alpha > 10^4$) cm⁻¹. This indicates that the transition takes place between the extended levels in the valence band and the extended levels in the conduction band. We also notice an increase in the values of the absorption coefficient with decreasing thickness at high optical energies, at low optical energies we notice a great convergence in the values of the absorption coefficient, and this is what we also observed in the absorbance. Likewise, the absorbance values converge greatly at high wavelengths. This is what researchers agreed upon²⁹ and³¹. Likewise, the researcher³².

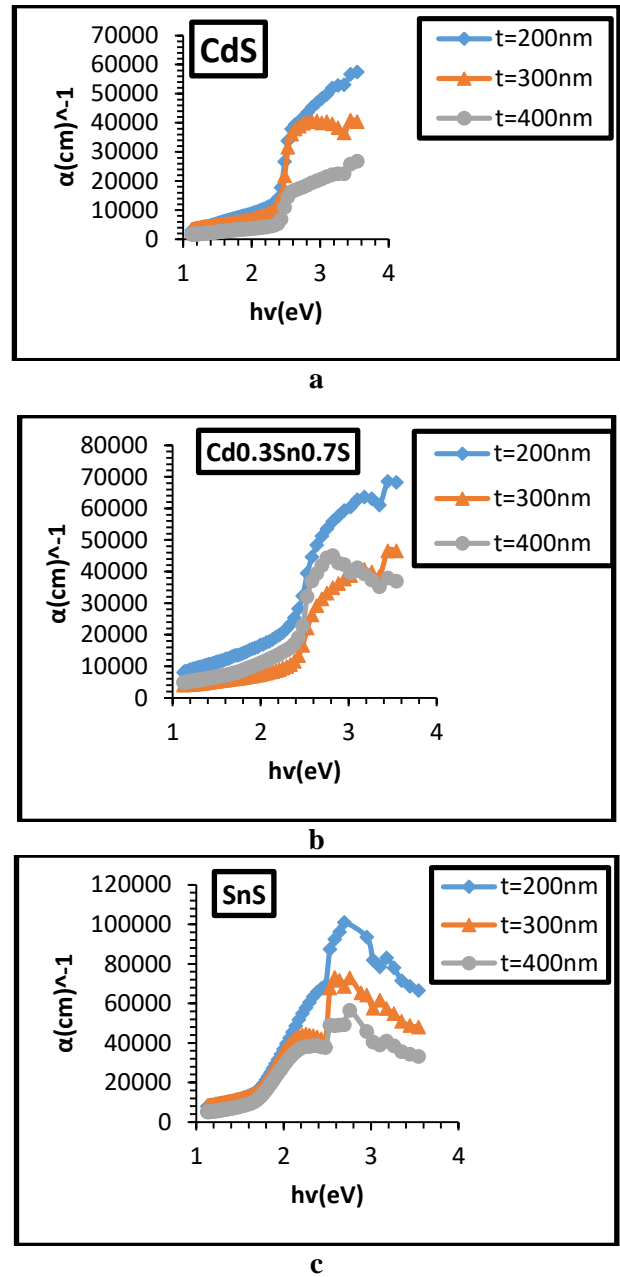


Figure 5. absorption coefficient spectra of (a)CdS ,(b)Cd_{0.3}Sn_{0.7}S ,(c)SnS Nanocrystalline thin films with different thicknesses.

The optical band gap energy values of the Cd_{1-x}Sn_xS films have been evaluated using the relation between absorption coefficient (α) and incident photon energy (hv) by using Tauc eq.³³:

$$\alpha h\nu = B_0(h\nu - E_g)^r \dots\dots 2$$

Fig. 6 and Table 3 show the variation of energy band gap of Cd_xSn_{1-x}S Nanocrystalline thin films with thickness and concentration of Sn

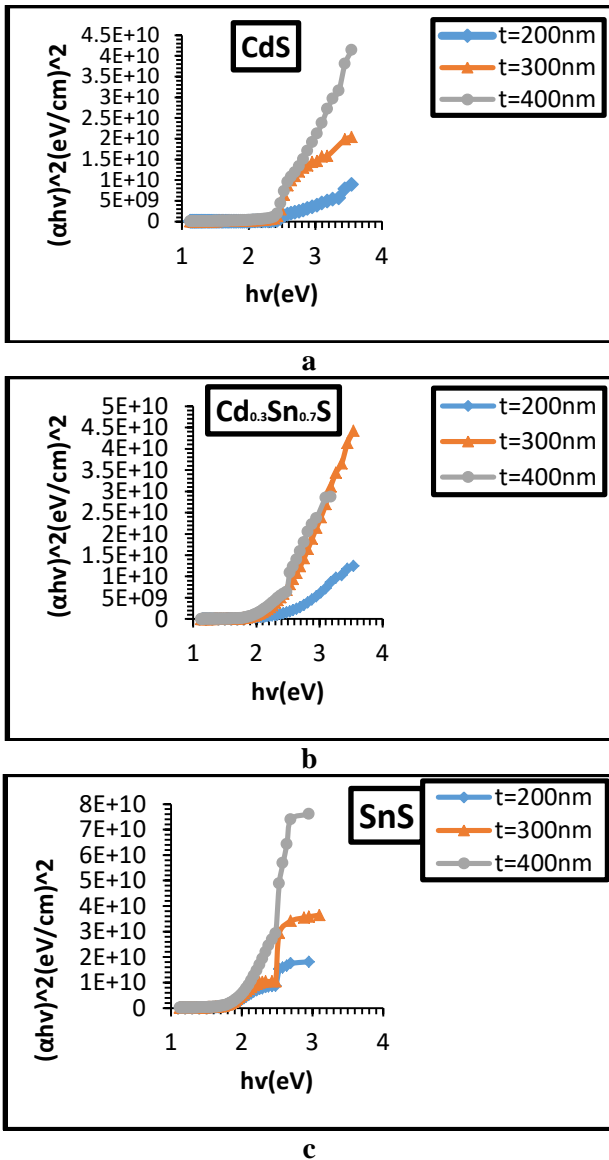


Figure 6. plots of $(\alpha hv)^2$ versus photon energy (hv) of (a) CdS, (b) Cd_{0.3}Sn_{0.7}S, (c) SnS Nanocrystalline thin films with different thicknesses.

Table 3. Variation of energy band gap of Cd_xSn_{1-x}S Nanocrystalline thin films with thickness and concentration of Sn

| X | Thickness t (nm) | Band gaps Eg (eV) |
|-----|------------------|-------------------|
| 0 | 200 | 2.48 |
| | 300 | 2.41 |
| | 400 | 2.3 |
| 0,7 | 200 | 2.26 |
| | 300 | 2.15 |
| | 400 | 1.92 |
| 1 | 200 | 1.95 |
| | 300 | 1.89 |
| | 400 | 1.87 |

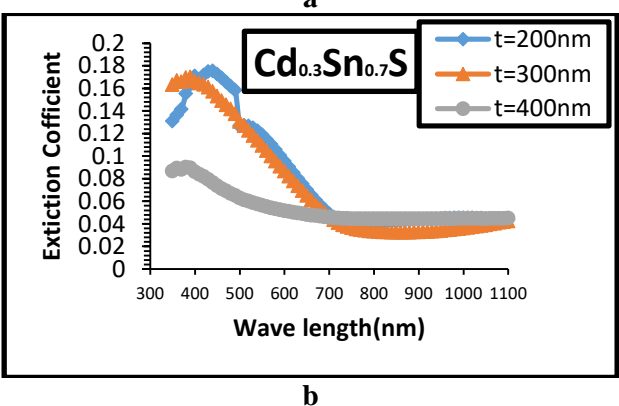
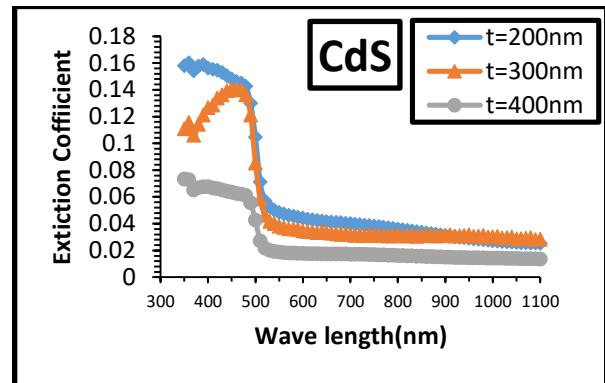
Fig. 6 and Table 3 show the variation of the energy band gap of Cd_xSn_{1-x}S Nanocrystalline thin films with the thicknesses of the films and concentration of Sn. It was found that the optical energy gap values decrease with increasing thickness and also with increasing Sn concentration.

The extinction coefficient (k_0) has been determined by using the following equation³⁴:

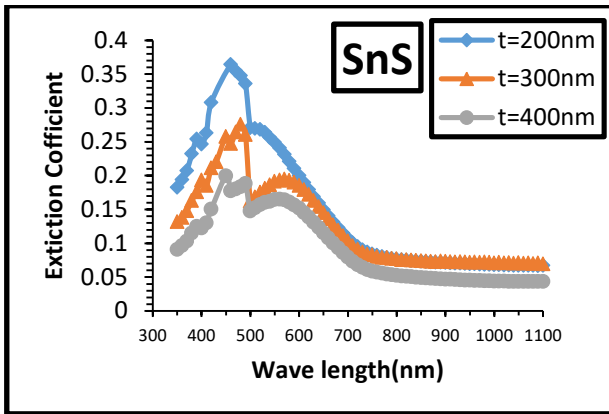
$$K_0 = \alpha \lambda / 4\pi \dots\dots\dots 3$$

Where, α : is the absorption coefficient and λ : is the wavelength of the incident photon.

It is clear from this equation that k_0 depends on α and has a similar behavior to α . Fig. 6, illustrates the variation of the extinction coefficient of Cd_{1-x}Sn_xS thin films with the wavelength for x (=0,0.7,1). From the figure, it is noted that the extinction coefficient changes with the change in thickness. The figure notes that the relationship is inverse between the extinction coefficient and the thickness, as the extinction coefficient increases with the increase in thickness, because the extinction coefficient behaves the same way as the absorption coefficient, and this is consistent with the results of the researcher²⁹. Likewise, the researcher³¹, and also the researcher³².



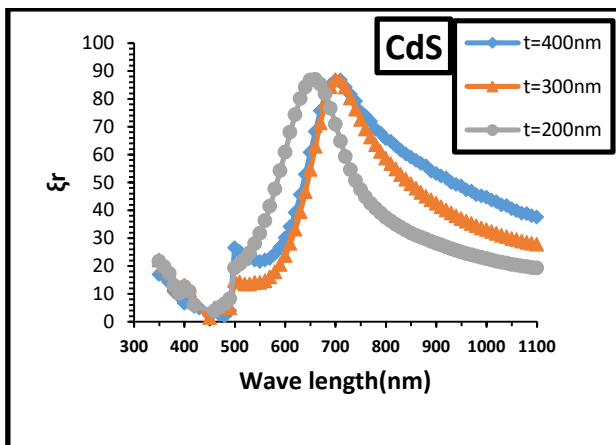
b



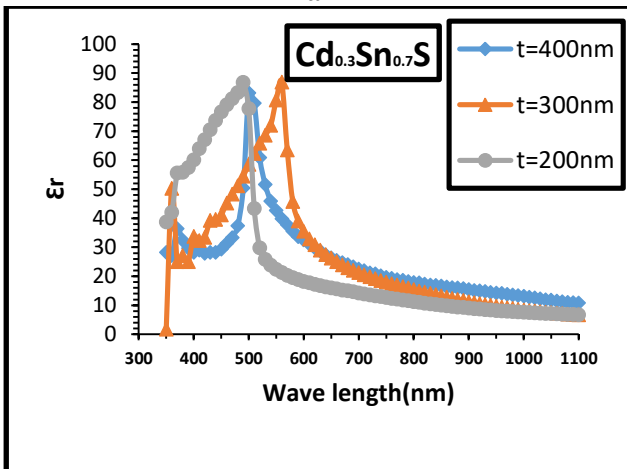
c

Figure 7. Extinction coefficient as a function of (a)CdS ,(b)Cd_{0.3}Sn_{0.7}S ,(c)SnS Nanocrystalline thin films with different thicknesses.

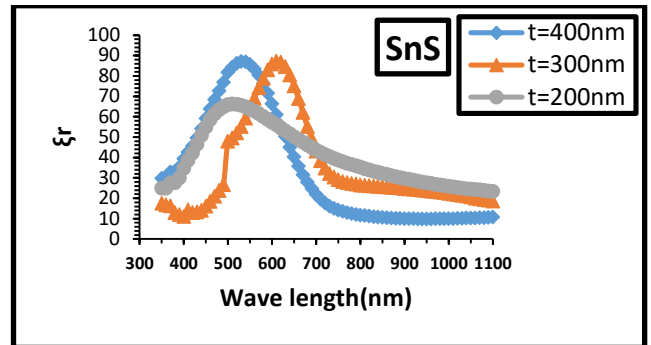
The variation of the real (ϵ_r) and imaginary (ϵ_i) parts of the dielectric constant values versus wavelength for Cd_{1-x}Sn_xS films deposited at R.T with different thicknesses are shown in Figs. 8, 9.



a

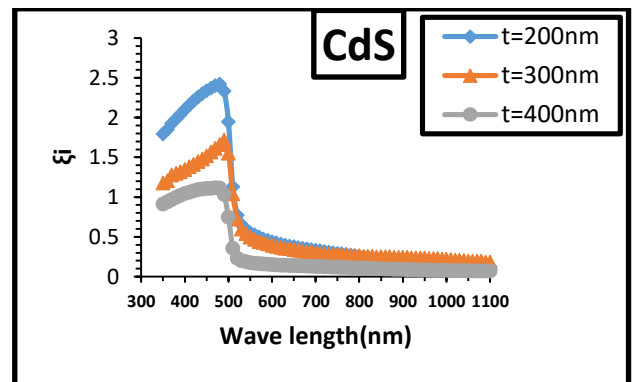


b

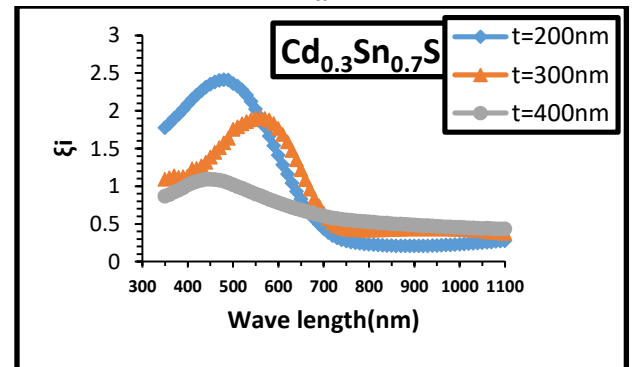


c

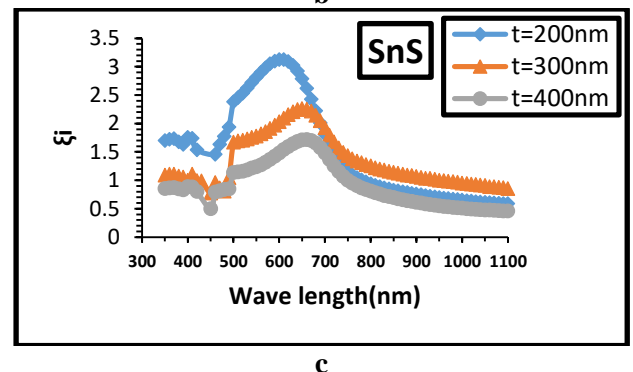
Figure 8. optical real constant(ϵ_r) of (a)CdS ,(b)Cd_{0.3}Sn_{0.7}S ,(c)SnS Nano crystalline thin films with different thicknesses.



a



b



c

Figure 9. optical dielectric constant (ϵ_i) of (a) CdS, (b) Cd_{0.3}Sn_{0.7}S, (c)SnS Nanocrystalline thin films with different thicknesses

Conclusion

To prepare the $Cd_{1-x}Sn_xS$ nanocrystalline films use first the participant method then use the chemical spray pyrolysis method at $300^\circ C$ substrate temperature. Films have been characterized using optical and structural measurements. XRD patterns of the films by found polycrystalline. Optical studies indicate that $Cd_{1-x}Sn_xS$ thin films exhibit a direct band gap which strongly depends on the Sn concentration and the thickness of the prepared nanocrystalline films. It was found that the optical energy gap values decrease with increasing the Sn

concentrations and with thickness. From the results obtained, it is clear that the prepared material can be used to manufacture the solar systems in taking into account the efficiency of the solar system, whether it is a solar thermal collector or a solar cell which are used as building facades, as well make the other tests to study the possibility of using the prepared samples in the manufacture of the sensors and the effect of changing thickness on the parameters of the gas sensors.

Acknowledgment

Write your acknowledgment here using the same text format.

Author's Declaration

- Conflicts of Interest: None.
- I hereby confirm that all the Figures and Tables in the manuscript are mine. Furthermore, any Figures and images, that are not mine, have been included with the necessary permission for

- re-publication, which is attached to the manuscript.
- Ethical Clearance: The project was approved by the local ethical committee in University of Baghdad.

References

1. Ahmet T, Tahsin K, Yusuf S. Structural and optical properties of Solar cells fabricated by spray pyrolysis deposited Cu_2CdSnS_4 thin films. *Renew Energ.* February 2020; 146: 1465-1470. <https://doi.org/10.1016/j.renene.2019.07.057>
2. Nada K, Lamia A, Suaad A. Effect Of Thickness On Structural And Optical Properties Of $ZnxCd_{1-x}S$ Thin Films Prepared By Chemical Spray Pyrolysis. *Int J Thin Film Sci Technol.* 2013; 2(2). Article 8.
3. Laura A C, José F, Abimael J, José E, Amanda C. Study of CdS/CdS Nanoparticles Thin Films Deposited by Soft Chemistry for Optoelectronic Applications. *Micromachines.* 2023; 14(6): 1168; <https://doi.org/10.3390/mi14061168>
4. Meshram RS, Suryavanshi BM, Thombre R.M. Structural and optical properties of CdS thin films obtained by spray pyrolysis. *Adv Appl Sci Res.* 2012; 3(3): 1563-1671. <https://doi.org/10.36648/0976-8610.14.2.11>
5. Jae Y, Soumyadeep S, Myeng G, Jaeyeong H. Controlled thickness of a chemical-bath-deposited CdS buffer layer for a SnS thin film solar cell with more than 3% efficiency. *J Alloys Compd.* 2019; 796: 160-166. <https://doi.org/10.1016/j.jallcom.2019.05.035>
6. Hakeem HS, Abbas NK. Preparing and studying structural and optical properties of $Pb_{1-x}Cd_xS$ nanoparticles of solar cells applications. *Baghdad Sci J.* 2021; 18(3): 640. <https://doi.org/10.21123/bsj.2021.18.3.0640>
7. Contreras JI, Díaz Flores A, Lozada R, Álvarez R, Balderas AJ. Structural and optical modifications of CdS properties in CdS -Au thin films prepared by CBD. *Results Phys.* 2021; 22: 103914. <https://doi.org/10.1016/j.rinp.2021.103914>
8. Wojciech Z, Agnieszka R, Anita TZ. Rational Design of the Electronic Structure of CdS Nanopowders. *Inorg Chem.* 2023; 62: 10955–10964. <https://doi.org/10.1021/acs.inorgchem.3c00935>
9. Mrinmoy D, Maitry D, Nipu K D, Ashoke Kumar Sen Gupta, Md Sharafat H, Mahmud M, et al. Deposition of CdS Thin Film by Thermal Evaporation. *Int Conf Electr Comput Commun Eng.* 2019. at Cox's Bazar, Bangladesh. <http://dx.doi.org/10.1109/ECACE.2019.8679325>
10. Abdelhamid S, Sameh E, Mohamed A, Omar K, Talaat M, Samy A. Influence of Deposition Time on Structural, Morphological, and Optical Properties of CdS Thin Films Grown by Low-Cost Chemical Bath Deposition. *Crystals.* 2023; 13(5): 788 <https://doi.org/10.3390/cryst13050788>
11. Zainab Y, Nada KA. Green synthesis of $CdS:Sn$ NPs by Starch as a Covering Agent and Studying its Physical Properties. *Baghdad Sci J.* 2023.

- <https://dx.doi.org/10.21123/bsj.2023.7290>
12. Rodríguez LA, Jose E, Ivonne L A , Jose C .Synthesis of π -SnS thin films through chemical bath deposition: effects of pH, deposition time, and annealing temperature. *J Mater Sci Mater Electron*. 2021; 32(6): 7464-7480. <https://doi.org/10.1007/s10854-021-05459-8>
 13. Visakh V M, Akshaya KC, Vijayakumar KP . Fabrication of p-type and n-type SnS thin films through vacuum-free deposition techniques. *Mater Today: Proceedings*.2023; <https://doi.org/10.1016/j.matpr.2023.02.104>
 14. Biswajit G ,Rajarshi R ,Sumit C ,Pushan B ,Subrata D.Synthesis of SnS thin films via galvanostatic electrodeposition and fabrication of CdS/SnS heterostructure for photovoltaic applications . *Appl Surf Sci*.. 2010; 256(13): 4328-4333. <http://dx.doi.org/10.1016/j.apsusc.2010.02.025>
 15. Tulay O, Sabiha A, Salih K. Vibrational and morphological properties of Sn-doped CdS films deposited by ultrasonic spray pyrolysis method . *Mater Sci Semicond Processing*. 2010; 13(5-6): 325-328. <http://dx.doi.org/10.1016/j.mssp.2011.02.013>
 16. Ogah E. O, Kotte R, Guillaume Z, Ian F, Robert W M. Annealing studies and electrical properties of SnS-based solar cells. *Thin Solid Films*. 2011; 519(21): 7425-7428. <https://doi.org/10.1016/j.tsf.2010.12.235>
 17. Guneri E, Ulutas C, KirmizigulF ,Altindemir G , Gode F, Gumus C. Effect of deposition time on structural, electrical , and optical properties of SnS thin films deposited by chemical bath deposition . *Appl Surf Sci*.. 2010; 257(4): 1189-1195. <https://doi.org/10.1016/j.apsusc.2010.07.104>
 18. Calixto RM , Martinez H , Sanchez JA , CamposA, Tiburcio SA , Calixto ME. Structural ,optical ,and electrical properties of tin sulfide thin films grown by spray pyrolysis .*Thin Solid Films*. 2009; 517(7): 2497-2499. <http://dx.doi.org/10.1016/j.tsf.2008.11.026>
 19. Turan E , KulM , Aybek AS , Zor M . Investigations In Structural Morphological And Optical Properties Of Cd 1-x Sn x S Thin Films . *Int J Thin Film Sci Technol*. 2020; 09(2): 89. <http://dx.doi.org/10.18576/ijtfst/090202>
 20. Cruz JS , Perez RC, DelgadoGT , AngelOZ. CdS thin films doped with metal-organic salts using chemical bath deposition. *Thin Solid Films*. 2010; 518(7): 1791-1795. <https://doi.org/10.1016/j.tsf.2009.09.034>
 21. Sudipto S. A Status Review on Cu₂ZnSn(S, Se)₄-Based Thin-Film Solar Cells. *Int J Photoenergy* . 2020 ; Article ID 3036413. <https://doi.org/10.1155/2020/3036413>
 22. Hosein K, Amin R B. Electrochemically deposited nanostructured Cd-doped SnS thin films: Structural and optical characterizations. *Ceram Int*. 2023.<https://doi.org/10.1016/j.ceramint.2023.11.354>
 23. Aimi Y, Takashi K, Yoji A, Shigeyuki N, Hiroto O, Hironori K, et al .Influence of Sn/S composition ratio on SnS thin-film solar cells produced via co-evaporation method24-K. *Jpn J Appl Phys*. 2018; 57(252). <https://doi.org/10.7567/JJAP.57.02CE08>
 24. Youssef N, Bouchaib H, Hicham L, Ahmed Z, Amine B, Abdelkrim B et.al. Synthesis of tin monosulfide SnS thin films via spray pyrolysis method based on Taguchi design for solar absorber. *Opt Mater*. 2022; 131: 112669.<https://doi.org/10.1016/j.optmat.2022.112669>
 25. Youssef N, Bouchaib H, Hicham L, Ahmed Z, Amine B, Abdelkrim B,et al. Synthesis of tin monosulfide SnS thin films via spray pyrolysis method based on Taguchi design for solar absorber. *Opt Mater*. 2022; 131: 112669. <https://doi.org/10.1016/j.optmat.2022.112669>.
 26. Cullity B D, Stock S R. Elements of x-ray diffraction. 3 rd ed., Prentice Hall, New york, 2001.
 27. Ilican S, CaglarY, Caglar M, Yakuphanoglu F. Structural, optical and electrical properties of F-doped ZnS nanorod semiconductor thin films deposited by sol-gel process. *Appl Sur Sci*. 2008; 255: 2353-2359. <http://dx.doi.org/10.1016/j.apsusc.2008.07.111>
 28. Aadim K, Ibrahim A, Marie J. Structural and optical properties of PbS thin films deposited by pulsed laser deposited (PLD) technique at different annealing temperature. *Int J Phys*. 2017; 5(1): 1-8. <https://doi.org/10.12691/ijp-5-1-1>
 29. Ziaul R K, Zulfequar M, Effect of thickness on structural and optical properties of thermally evaporated cadmium sulfide polycrystalline thin films. *Chalcogenide Lett*. 2010; 7(6): 431-438 . https://chalcogen.ro/431_Raza-Khan.pdf
 30. Shaker DS, Abass NK, Ulwall RA. Preparation and study of the structural, morphological and optical properties of pure tin oxide nanoparticle doped with Cu. *Baghdad Sci J*.,2022; 19(3): 660–669. <https://doi.org/10.21123/bsj.2022.19.3.0660>
 31. Kathirvela N, Suriyanarayanan N, Suriyanarayanan S, Prabahar S. Structureal .electrical and optical properties of CdS thin films by vacuum evaporation deposition . *J Ovonic Res*. 2011; 7(4): 83-92.
 32. Nwofe PA, Ramakrishna KT,. Tan JK, Forbes I, Miles RA. Thickness Dependent Optical Properties of Thermally Evaporated SnS Thin Films. *Phys Procedia*.2012; 25: 150-157. <https://doi.org/10.1016/j.phpro.2012.03.064>
 33. Francisco T, Leitão M A , MirandaMarcus A R ,Miranda C, Morilla-Santos C, Morilla S M, et.al. The Scherrer equation and the dynamical theory of X-ray diffraction. *Acta Crystallogr Found Adv*. 2016; 72(3). <http://dx.doi.org/10.1107/S205327331600365X>
 34. Khan ZR, Zulfequar M, Khan NS. Effect of thickness on structural and optical properties of thermally evaporated cadmium sulfide

تأثير السماكة على الخصائص الهيكلية والمورفولوجية والبصرية للأغشية الرقيقة النانوية من Cd_{1-x}Sn_xS للتطبيقات الإلكترونية البصرية

لمياء خضير عباس

قسم الفيزياء، كلية العلوم، جامعة بغداد، بغداد، العراق.

الخلاصة

تتم تحضير أغشية رقيقة من البلورات النانوية Sn_{1-x}Cd_xS (x=0,0.7, and 1) بسماكات مختلفة (200، 300، 400) نانومتر على قواعد زجاجية عند درجة حرارة 300 درجة مئوية بطريقة المشاركة وطريقة الانحلال الحراري بالررش الكيميائي (CSP). تمت دراسة تأثير تركيز Sn والسماكة على الخصائص التركيبية والبصرية للأغشية المحضرة. تم توصيف الأغشية لتقييم البنية والنفاذية وفجوة نطاق الطاقة الضوئية. أظهرت دراسات حيود الأشعة السينية (XRD) أن الأفلام كانت متعددة البلورات ذات هياكل سداسية ومتعامدة. أظهرت نتائج الأشعة السينية وقياس القوة الذرية أن حجم الحبيبات يزداد مع سماكتها. تم تحديد طاقات فجوة النطاق البصري ونوع الانتقال والامتصاص البصري للأغشية من أطراف النفاذية البصرية. أظهرت دراسات الامتصاص البصري في مدى الطول الموجي (200-1100 نانومتر) أن قيم طاقة فجوة الطاقة للأغشية تتناقص من (1.95-2.48) إلكترون فولت، (1.92-2.41) إلكترون فولت، و(1.89-2.3) إلكترون فولت مع زيادة تركيز القصدير ومع زيادة السماكة (200، 300، 400) نانومتر على التوالي. تم تحديد أفضل خواص للمادة المحضرة لإمكانية استخدامها في صناعة الخلايا الشمسية.

الكلمات المفتاحية: بلورات Sn_{1-x}Cd_xS، الانحلال الحراري بالررش الكيميائي، جسيمات CdS النانوية، جسيمات SnS النانوية، الأغشية الرقيقة.